New Journal of Chemistry

Electronic Supplementary Information for

Synthesis and Gas Sorption Behaviour of ZIF-90 with Large Pore Volume

*Paola F. Liguori, Beatrice Russo, Alessandro Melicchio and Giovanni Golemme**

Dipartimento di Ingegneria per l'Ambiente e il Territorio e Ingegneria Chimica, Università della Calabria, via P. Bucci 45/A, 87036 Rende, Italy

Corresponding author's e-mail address: giovanni.golemme@unical.it

Van der Waals volumes of ZIF-8 and ZIF-90

The composition of the sodalite unit cell of both ZIF-90 and of ZIF-8 is $[Im_2Zn]_{12}$,[1,2] where Im is the imidazolate-2-carboxaldehyde (ICA^-) for ZIF-90, or the 2-methylimidazolate (mIm^-) anion (ZIF-8). The difference in the van der Waals volumes of the two ZIFs is determined by the difference in the volumes of the methyl and of the aldehydic groups. According to Bondi,[3] the van der Waals volume of a methyl group is 13.67 cm^3mole^{-1}, the one of a –CHO group is 14.22 cm^3mole^{-1}: the latter is 0.55 cm^3mole^{-1} (or 0.91 $Å^3$) larger than the former. Therefore the van der Waals volume of ZIF-90 is 22 $Å^3$/uc larger than that of ZIF-8.

Materials

Imidazole-2-carboxaldehyde (H-ICA, 98%, Conier Chem & Pharma Ltd., PRC), methanol (VWR, 100%), zinc nitrate hexahydrate (≥99.0%) and triethylamine (≥99.5%), both from Sigma Aldrich, were used as received without further purification. Ultra-pure grade gases (99.999% or higher purity, Sapio, Italy) were used for sorption experiments.

Synthesis of ZIF-90

To a solution of H-ICA (0.6985 g, 0.00719 mol) in 30 mL of methanol, 0.727 g (0.00719 mol) of triethylamine (TEA) were added. The resulting solution was stirred at room temperature for 5 minutes. Then, a solution of $Zn(NO_3)_2 \cdot 6H_2O$ (1.0672 g, 0.00359 mol) in 30 mL of methanol was added. The resulting mixture was stirred under reflux at 70 °C for 4 min. The white precipitate was filtrated out, washed with methanol to give the pure ZIF-90 as a white powder. The resulting crystals were dried overnight at 110 °C. Yield was 98% based on Zn.

SEM, XRD and thermogravimetric characterizations

Scanning electron micrographs (FEG Quanta 200 Environmental SEM, FEI Philips) were recorded after sputtering the sample with graphite. The powder X-ray diffraction pattern was obtained at room temperature by using a Bruker D2 PHASER Diffraction System equipped with a 1D high speed solid state LinxEye detector and Cu-K_α radiation (λ = 1.54056 Å), in the 2θ range 0.5–40° with steps of 0.005° and a count time of 1.5 sec per step. Thermogravimetric analysis (TGA) was performed on a Pyris 6 TGA (Perkin Elmer): 6.0 mg samples were filled into a crucible heated under nitrogen from 30 to 800 °C at a rate of 10 °C/min.

FT-IR and Raman Spectra

Infrared spectra (KBr) in the range 4000–400 cm^{-1} were recorded on a Spectrum One FT-IR spectrometer (Perkin Elmer) (Figure S1).

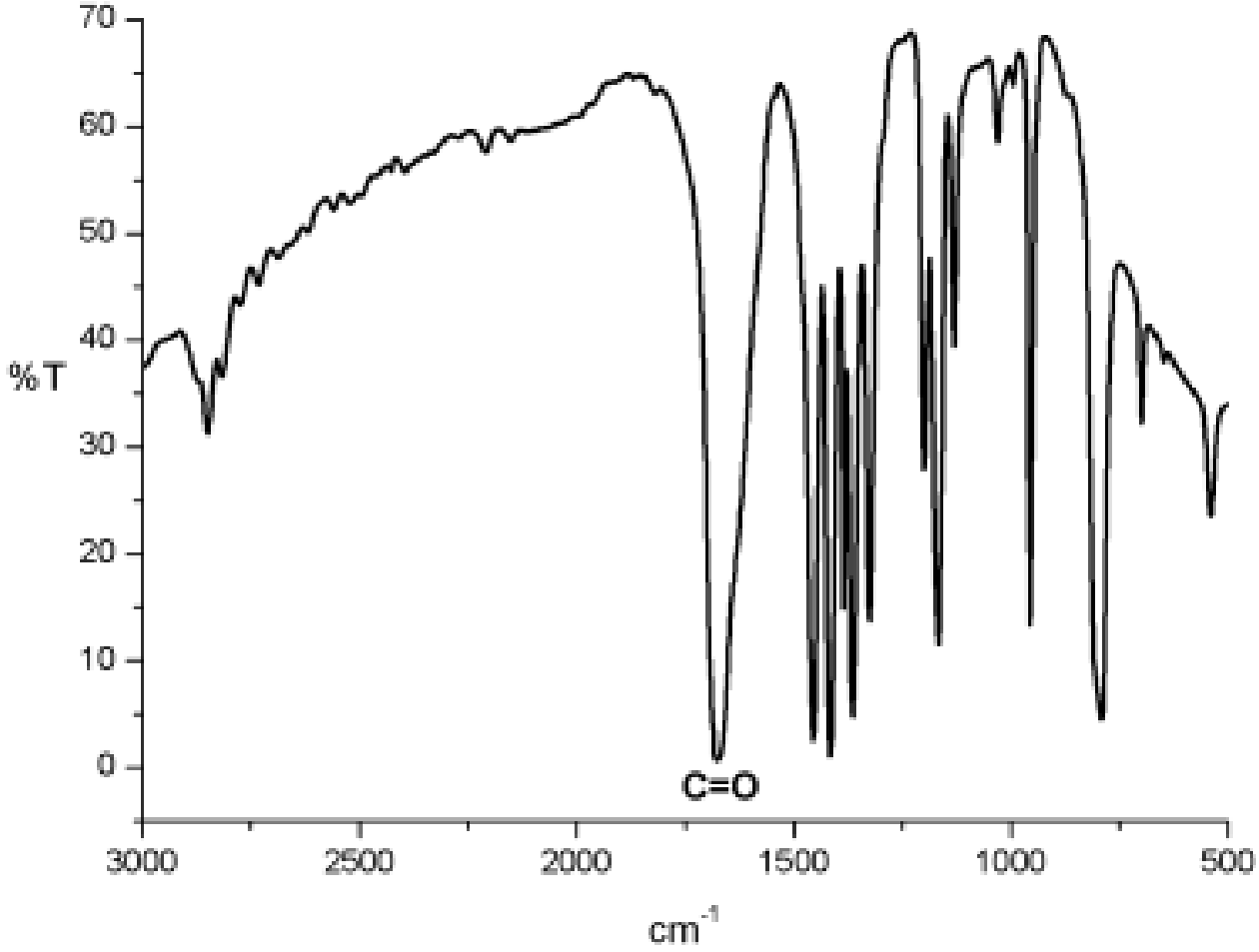

Figure S1. FT-IR spectrum of ZIF-90.

The Raman spectrum (Fig. S2) was recorded from 1000 to 3200 cm^{-1} Raman shift, at room temperature, using a NRS-5100 Raman micro-spectrometer (Jasco Analytical Instruments, Japan) with laser power of 1.5 mW of the 532.11 nm line of a SOC frequency-doubled Nd:YAG (Showa Optronics Co. Ltd, Japan) for excitation.

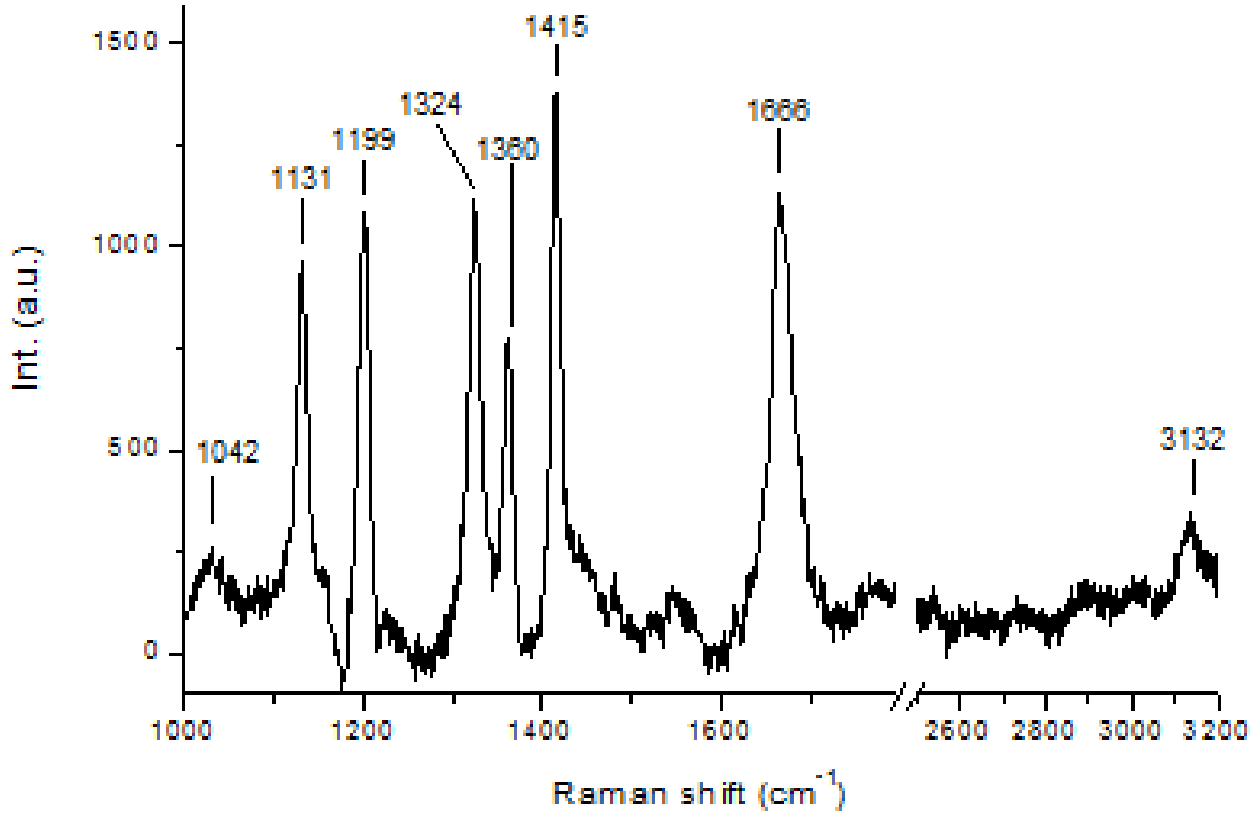

Figure S2. Raman spectrum of ZIF-90.

Table S1. Assignments of Raman peaks of ZIF-90; vs: very strong; s: strong; m: medium; w: weak; ν: stretching; δ: in-plane bending [4-6].

Raman shift (cm^{-1})	Intensity	Assignments
3132	w	ν CH ring
1666	vs	ν CO + δ CCH + δ CN
1415	s	δ CCH +ν CC +ν CN
1360	m	ν CN + δ COH + δ CCH
1324	m-s	δ CH + ν CN
1199	m-s	ν CN + ν CC
1131	m-s	δ NCH + δ CCH + ν CN ring + δ CCN
1042	w	δ CH

Gas Sorption analysis

Ar (87.45 K), N_2 and H_2 (77.35 K) isotherms were measured on an Autosorb iQ MP XR (Quantachrome) equipped with a Cryocooler. Prior to the measurements ZIF-90 was degassed at 150 °C for 16 h under vacuum. CH_4 isotherm was obtained at 273.15 K with a Tristar 3020 II (Micromeritics). Prior to the measurement the sample was degassed at 150 °C for 16 h under N_2 flow. The calculated BET specific surface areas satisfy the four Rouquerol consistency criteria [7,8] for both N_2 and Ar (Figure S3 and Table S2). The plots in Figures S3a) and S3b) have been used to select the maximum p/p_0 value for the calculation of the BET specific surface area of ZIF-90 according to the first Rouquerol consistency criterion. The plots in Figures S3c) to S3h) have been used to evaluate the linearity of the BET plots. The monolayer loadings (N_m) correspond to $(p/p_0)_m$ values falling within the selected linear regions; the $(p/p_0)_m$ values differ from the monolayer loadings calculated from the BET theory of less than 20%. The total micropore volume (MV) is calculated from the monolayer loading via the densities of liquid Ar (1.400 g/cc) and of liquid N_2 (0.808 g/cc).

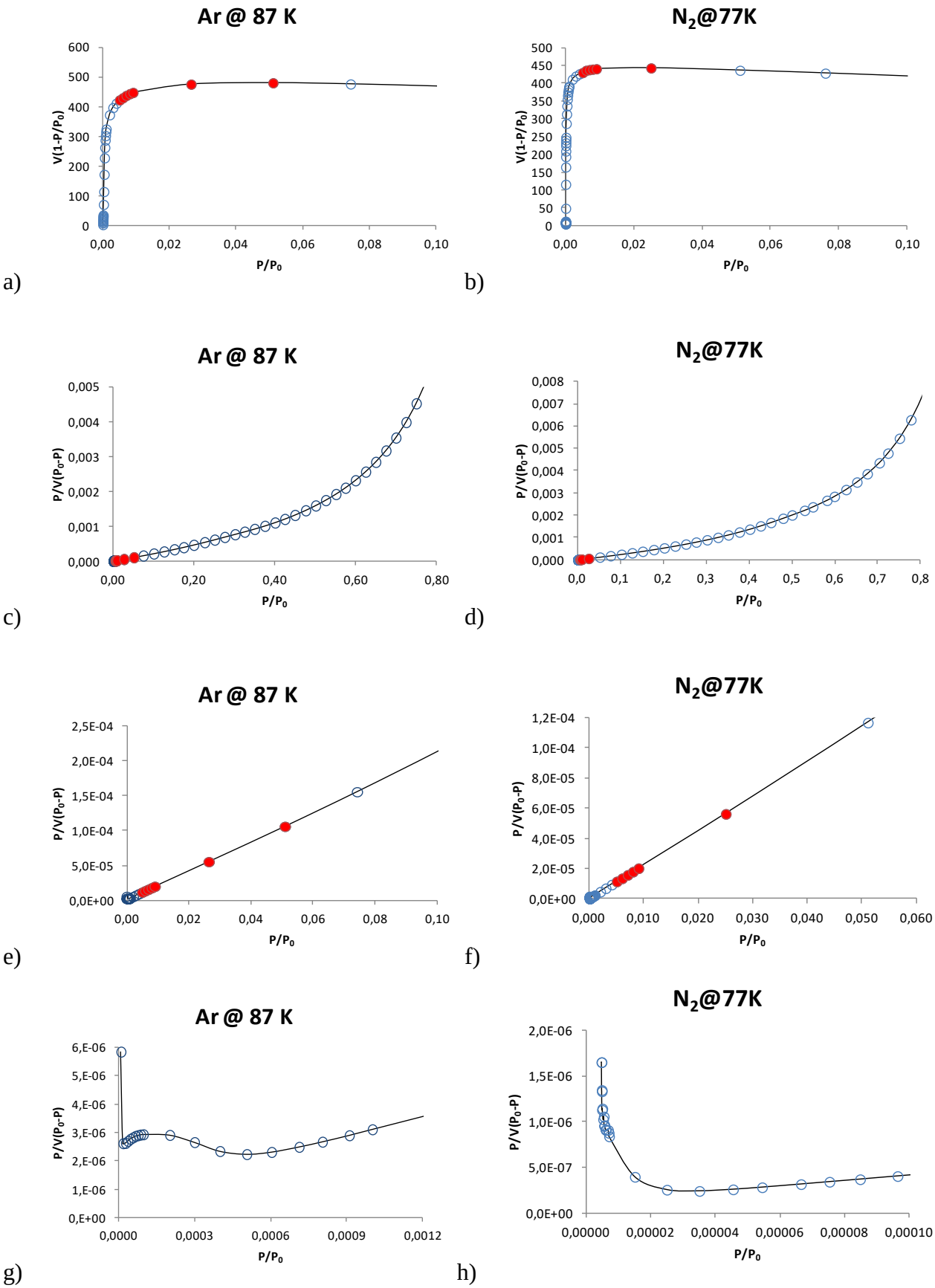

Figure S3. Plots used to select the maximum p/p_0 value for the BET specific surface area of ZIF-90 according to the first Rouquerol consistency criterion (a, c), and BET representation of gas isotherms (c-h). The points selected for the workout of the BET values are highlighted in red.

Table S2. Langmuir (S_L) and BET (S_B) surface areas [m^2g^{-1}] with correlation coefficients (R_L, R_B) of the linear fittings; BET C constants; monolayer loadings (N_m) and relative pressures ($(p/p_0)_m$); monolayer relative pressures calculated from BET theory ($1/(1+\sqrt{C})$); and micropore volume (MV) at the monolayer pressure [cm^3g^{-1}]

Gas	S_L	R_L	S_B	R_B	C	N_m, cm^3g^{-1}	$(p/p_0)_m$	$1/(1+\sqrt{C})$	MV
Ar	1971	1.0000	1859	0.999996	1257.7	487.37	$2.592\ 10^{-2}$	$2.742\ 10^{-2}$	0.620
N_2	2000	1.0000	1937	0.999992	7909.6	445.07	$9.497\ 10^{-3}$	$1.112\ 10^{-2}$	0.688

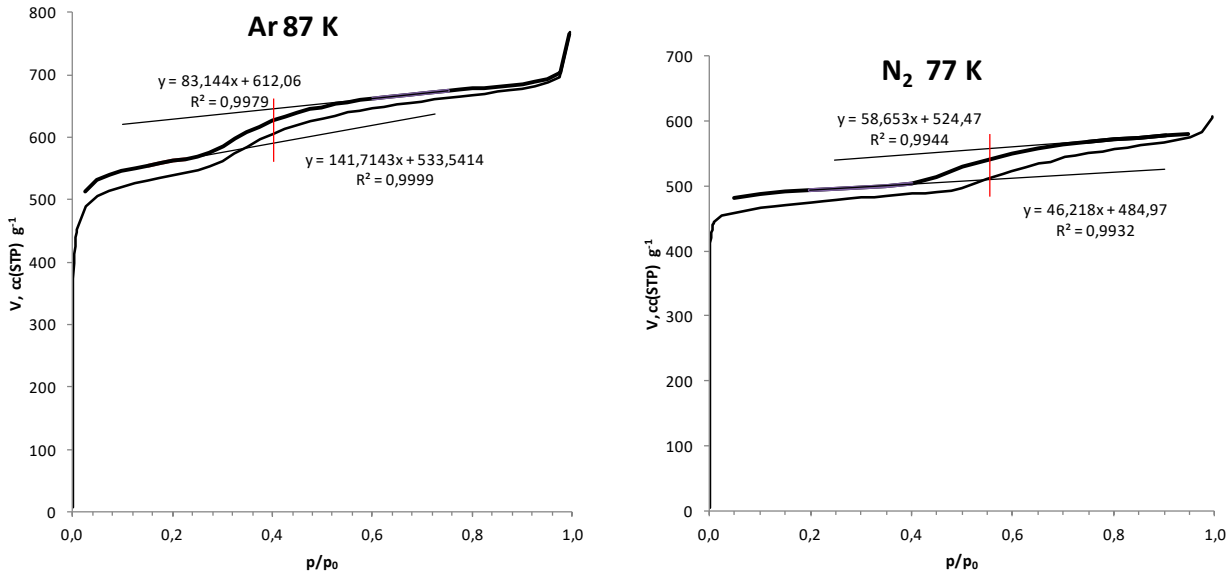

Figure S4. Ar and N_2 adsorption/desorption isotherms on ZIF-90. The additional amount of gas adsorbed in the pores of ZIF-90 around the pressure indicated by the red segment is evaluated from the desorption branch, as specified in the text.

The last step in the Ar and N_2 sorption/desorption isotherms (Fig. S4) is visible at relative pressures in excess of 0.22 and 0.47, respectively. In this range of pressures the pores of ZIF-90 are already filled, and the multi-layer adsorption around the crystals is responsible of the non-zero slope of the curves before and after these steps. In order to eliminate the contribution of multi-layer adsorption, the amount of each gas adsorbed at the jump is evaluated from the distance of the lines obtained from the best fit of the isotherm before and after the jump, as depicted in Fig. S4. At $p/p_0 = 0.40$, the middle of the jump, the distance between the lines is of 55.09 cc/g for Ar, equivalent to 7.53 molecules per unit cell. At $p/p_0 = 0.55$, the jump is of 46.34 cc/g for N_2, equivalent to 6.34 molecules per unit cell.

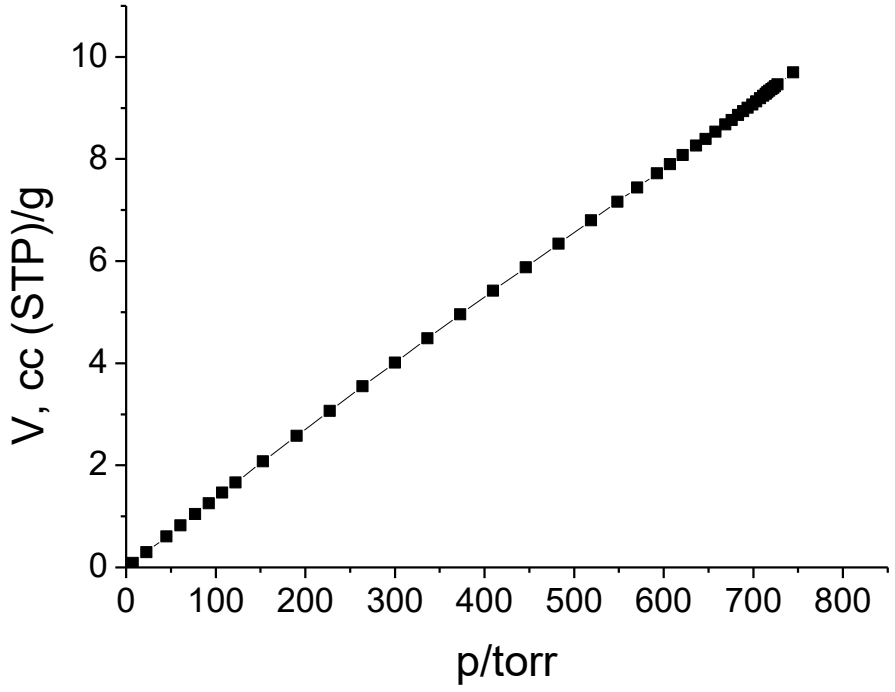

Figure S5. CH_4 adsorption isotherm at 273.15 K in ZIF-90.

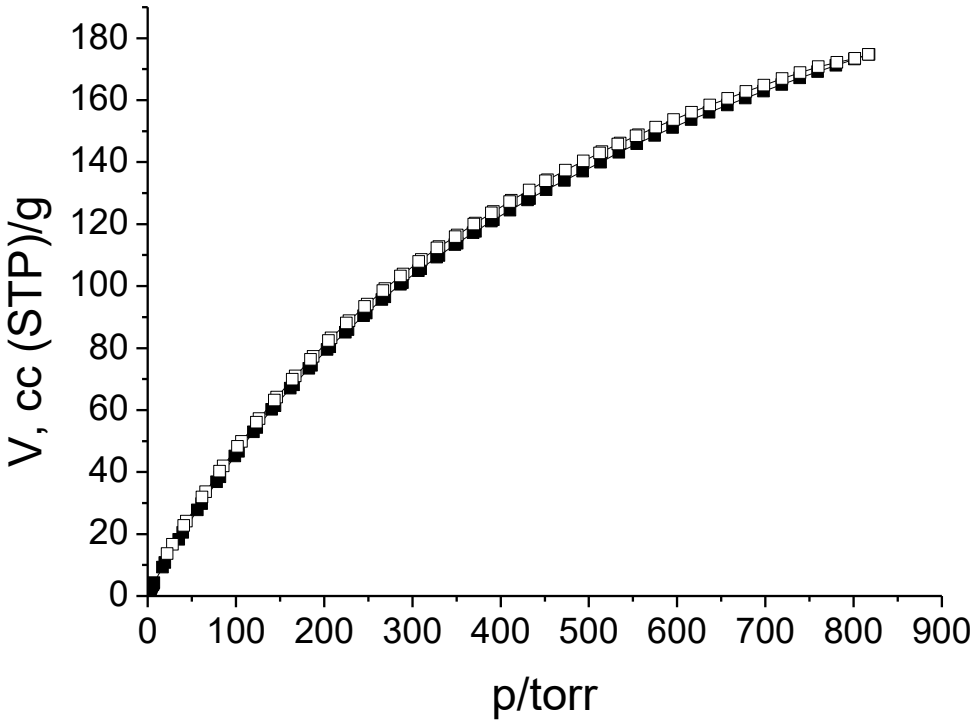

Figure S6. H_2 adsorption (bold squares) and desorption (empty squares) isotherms at 77.35 K in ZIF-90.

NLDFT Ar pore size distribution

The pore size distribution of ZIF-90 in Figure S7 is obtained from the Ar sorption isotherm at 87 K by using a NLDFT model suitable for rigid adsorbents. The swelling of the ZIF-90 lattice would give rise to fictitious peaks.

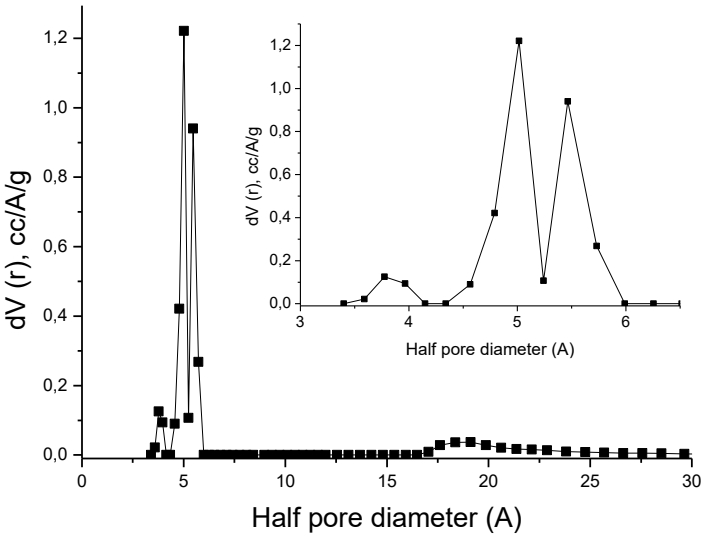

Figure S7. Pore Size Distribution of ZIF-90 obtained from the Ar adsorption isotherm at 87.45 K by means of the NLDFT model for zeolites and silica (cylindrical/spherical pores) available in the Quantachrome library of Autosorb® iQ XR MP.

References

1. Park K.S., Ni Z., Cote A.P., Choi J.Y., Huang R.D., Uribe-Romo F.J., Chae H.K., O'Keeffe M., Yaghi O.M., Exceptional Chemical and Thermal Stability of Metal-Organic Frameworks, *Proc. Natl. Acad. Sci. U.S.A.,* 2006, **103**, 10186.
2. Morris W., Doonan C.J., Furukawa H., Banerjee R., Yaghi O.M., Crystals as Molecules: Postsynthesis Covalent Functionalization of Zeolitic Imidazolate Frameworks, *J. Am. Chem. Soc.,* 2008, **130**, 12626.
3. Bondi A., van der Waals Volumes and Radii, *J. Phys. Chem.*, 1964, **68**, 441.
4. Socrates G., Infrared and Raman Characteristic Group Frequencies: Table and Charts, Wiley: Chichester, UK, 2001.
5. Nakamoto K., Infrared and Raman Spectra of Inorganic and Coordination Compounds, Wiley: Hoboken, NJ, 2009.
6. Polat T., Yurdakul S., *J. Mol. Struct*., 2013, **1053**, 27.
7. Rouquerol F., Rouquerol J., Singh K.S.W., Llewellyn P., Maurin G., Adsorption by Powders and Porous Solids, 2nd ed., Academic Press: Amsterdam (NL), (2014).
8. Gómez-Gualdrón D.A., Moghadam P.Z., Hupp J.T., Farha O.K., Snurr R.Q., Application of Consistency Criteria to Calculate BET Areas of Micro- and Mesoporous Metal−Organic Frameworks, *J. Am. Chem. Soc.*, 2016, **138**, 215.
9. Tian T., Wharmby M.T., Parra J.B., Ania C.O., Fairen-Jimenez D., Role of Crystal Size on Swing-Effect and Adsorption Induced Structure Transition of ZIF-8, *Dalton Trans.,* 2016, **45**, 6893.